Room temperature tunable detection of subterahertz radiation by plasma waves in nanometer InGaAs transistors

F. Teppe, M. Orlov, A. El Fatimy, A. Tiberj, W. Knap, J. Torres, V. Gavrilenko, A. Shchepetov, Y. Roelens, and S. Bollaert

Citation: Appl. Phys. Lett. **89**, 222109 (2006);
View online: https://doi.org/10.1063/1.2392999
View Table of Contents: http://aip.scitation.org/toc/apl/89/22
Published by the American Institute of Physics

Room temperature tunable detection of subterahertz radiation by plasma waves in nanometer InGaAs transistors

F. Teppe,[a)] M. Orlov,[b)] A. El Fatimy, A. Tiberj, and W. Knap
Groupe d'Etude des Semiconducteurs, CNRS-Université Montpellier 2, UMR 5650, 34090 Montpellier, France

J. Torres
Centre d'Electronique et de Micro-Optoélectronique de Montpellier, CNRS-Université Montpellier 2, UMR 5507, 34090 Montpellier, France

V. Gavrilenko
Institute for Physics of Microstructures, Russian Academy of Sciences, GSP-105, Nizhny Novgorod, 603950 Russia

A. Shchepetov, Y. Roelens, and S. Bollaert
Institut d'Electronique, de Microélectronique et de Nanotechnologie, UMR 8520, Cité Scientifique, Avenue Poincaré, BP 60069, 59652 Villeneuve d'Ascq Cedex, France

(Received 28 July 2006; accepted 13 October 2006; published online 29 November 2006)

The authors report on the demonstration of room temperature, tunable terahertz detection obtained by 50 nm gate length AlGaAs/InGaAs high electron mobility transistors (HEMTs). They show that the physical mechanism of the detection is related to the plasma waves excited in the transistor channel and that the increasing of the drain current leads to the transformation of the broadband detection to the resonant and tunable one. They also show that the cap layer regions significantly affect the plasma oscillation spectrum in HEMTs by decreasing the resonant plasma frequencies.
 [DOI: 10.1063/1.2392999]

Tuneable solid-state detectors are expected for the development of electronic and photonic applications in the terahertz part of the electromagnetic spectrum. There are a large variety of terahertz detectors such as bolometers,[1–3] pyroelectric detectors, Schottky diodes,[4,5] and photoconductive detectors.[6] Tunability has been demonstrated in photoconductivity measurements by applying magnetic field in GaAs (Ref. 7) and InSb.[8] Here we show the potential of terahertz detectors tuned by plasma wave resonances in field effect transistors (FETs). Tuning the detector response by gate voltage is much suitable for applications than tuning with a magnetic field.

The plasma waves in a FET have a linear dispersion law,[9] $\omega = sk$, where s, given in Eq. (3), is the plasma wave velocity, which depends on the square root of the gate voltage swing V_0. A FET channel of a given length L_g acts for these waves as a resonant "cavity," with the eigenfrequencies given by $\omega_N = \omega_0(1+2N)$, where $N = 1, 2, 3, \ldots$ and fundamental plasma frequency $\omega_0 = \pi s / 2L_g$ can be tuned by changing the gate voltage. For the submicron gate lengths ω_0 can reach the terahertz range.[10,11] Dyakonov and Shur[12,13] showed that nonlinear properties of such a cavity can be exploited for selective tunable terahertz detection. They demonstrated that a nanometer size high electron mobility transistor (HEMT) subjected to a terahertz radiation with a frequency ω would develop a constant source-to-drain voltage,

$$\Delta U \propto \frac{1}{(\omega - \omega_0)^2 + (1/2\tau)^2}, \tag{1}$$

where τ is the momentum relaxation time.

In the absence of external current the width of the resonance curve is determined mainly by the inverse momentum relaxation time, $1/\tau$. When $\omega_0 \tau \ll 1$ the plasma oscillations are overdamped and the HEMT response is a smooth function of frequency as well as of the gate voltage (nonresonant broadband detection). In the regime such that $\omega_0 \tau \gg 1$ the field effect transistor operates as a resonant and tunable detector. The fundamental frequency of plasma wave oscillations can be tuned by changing the gate voltage.

The resonant detection of terahertz radiation by two-dimensional plasma waves was demonstrated in different FETs (Refs. 14–16) and in a single and a double quantum well FET.[17,18]

Recently, Teppe *et al.* have demonstrated room temperature, resonant detection of subterahertz radiation by 250 nm gate length GaAs/AlGaAs transistor.[19] They have shown that the detection regime, initially nonresonant, becomes resonant even at 300 K by increasing the drain current and driving the transistor into the current saturation region.

In this letter we experimentally show that the resonant detection of subterahertz radiations can be continuously tuned by the applied gate voltage.

The experiments were performed on two 50 nm gate length AlGaAs/InGaAs HEMTs called later sample A and sample B. The active layers consisted of a 200 nm $In_{0.52}Al_{0.48}As$ buffer, a 15 nm $In_{0.7}Ga_{0.3}As$ channel, a 5-nm-thick undoped $In_{0.52}Al_{0.48}As$ spacer, a silicon δ layer of $5\ 10^{12}/cm^2$, a 12-nm-thick $In_{0.52}Al_{0.48}As$ barrier layer, and finally a 10-nm-silicon-doped $In_{0.53}Ga_{0.47}As$ cap layer. Cap layer length is 500 nm at each side of the channel and drain-source separation is 1.4 μm (see schematic in inset of Fig. 1). The threshold voltages extracted from transfer characteristics were −0.6 and −0.4 V for samples A and B, respectively. Output characteristics of sample B at room temperature (drain current I_d versus source-drain voltage V_d) for

[a)]Author to whom correspondence should be addressed; electronic mail: teppe@ges.univ-montp2.fr

[b)]Also at Institute for Physics of Microstructures, Russian Academy of Sciences, GSP-105, Nizhny Novgorod, 603950 Russia.

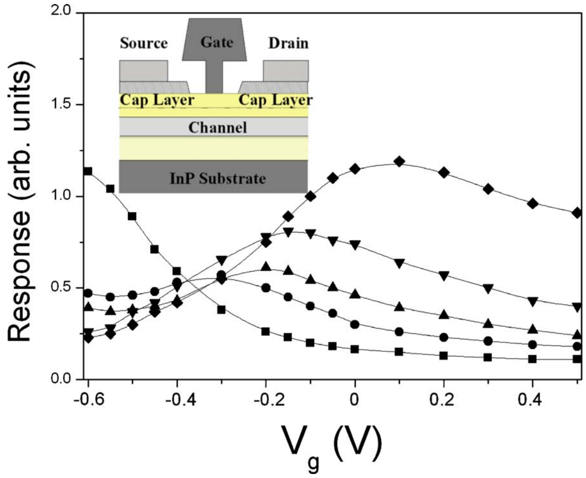

FIG. 1. (Color online) Photoconductive response vs gate voltage for different values of applied drain-source voltage V_d from 0.025 up to 0.55 V [(■): 0.025 V, (●): 0.2 V, (▲): 0.3 V, (▼): 0.4 V, and (♦): 0.55 V] at a fixed value of the BWO frequency of 663 GHz. For V_d=0.025 V typical nonresonant signal is observed. For higher V_d values the resonant peak starts to grow and shifts to higher values of gate voltage. Inset: schematic of the 50 nm gate-lenght InGaAs HEMTs that highlights cap layer regions.

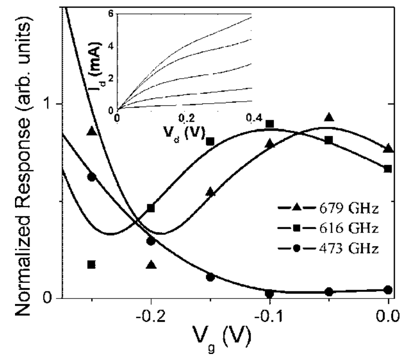

FIG. 2. Photoinduced drain-source voltage as a function of gate bias for different external frequencies [(▲): 679 GHz, (■): 616 GHz, and (●): 473 GHz] at a fixed value of applied drain-source voltage of 0.3 V. At the lowest frequency, the response is nonresonant. The resonance appears at V_g=0.1 V at 616 GHz and shifts to higher gate bias (0.05 V) for higher frequency (679 GHz). Inset: output characteristics at room temperature (drain current I_d vs source-drain voltage V_d) for different values of gate voltage (from 0 down to −0.4 V with −0.1 V step).

different values of gate voltages (from 0 down to −0.4 V with −0.1 V step) are displayed in the inset of Fig. 2. The photoresponse measurements were performed with backward wave oscillator (BWO) source which gives powerful and tunable subterahertz electromagnetic waves from 450 up to 700 GHz. The radiation beam was not focused and the diameter of the spot was approximately 5 cm at the position of the sample, i.e., much larger than the gate length of the device. The maximum BWO output power was around 20 mW. The radiation intensity was modulated by the mechanical chopper at 130 Hz. The source terminal of the device was grounded. The dc drain current was applied to the device and controlled by a Keithley source meter 2410. The source meter was operating in the current source mode, ensuring the asymmetry in the boundary conditions for the ac signal at the drain and source terminals. The dependence of the response ΔU versus the drain current was measured using the standard lock-in technique at different gate biases. The gate bias was controlled by another Keithley source meter operated in the voltage source mode.

Concerning sample A, the photoconductive response versus the gate voltage for different values of applied drain-source voltage V_d from 0.025 up to 0.55 V at a fixed value of the BWO frequency of 663 GHz is shown in Fig. 1. One can see that for V_d=0.025 V typical nonresonant signal is observed. The resonant peak appears at higher V_d, its amplitude increasing and its position shifting to higher values of gate voltage with the applied V_d. We want to point out that the plasma wave resonance appears as the transistor is driven into the current saturation region. This behavior was observed in sample B as well.

The photoconductive response of sample B versus gate voltage for frequencies from 473 up to 679 GHz is shown in Fig. 2 while keeping constant the source drain voltage of 0.3 V. One can see that for the lowest frequency, only typical nonresonant signal is observed. For higher frequencies, after a typical increase of the nonresonant background signal with applied drain voltage/current, the resonant structure starts to grow. Results shown in Figs. 1 and 2 show clearly that the resonant detection is obtained either by (i) increasing the relaxation time τ or by (ii) increasing external frequency ω. Both effects lead to increasing of the effective quality factor $\omega\tau$. As mentioned before $\omega\tau$ should be higher than unity to get resonant detection. As discussed in our earlier work,[19,20] increasing the current increases the electron drift velocity v and leads to the decrease of an effective relaxation rate given by $1/\tau_{\text{eff}}=1/\tau-2v/L_g$, L_g being the gate length. As $\omega\tau_{\text{eff}}$ becomes on the order of unity the detection becomes resonant.

The main experimental result shown in this letter is that the position of the resonance line shifts with external frequency. Figure 3 reports the experimentally observed variation of the maxima of the gate voltages for three different fixed drain-to-source voltages (0.1 V: triangles, 0.2 V: circles, and 0.3 V: squares). One can see that by increasing the external frequency of BWO the resonance shifts to higher gate voltages for different values of fixed source-drain voltage.

According to plasma wave detection theory the frequency of plasma wave oscillations f depends on the gate

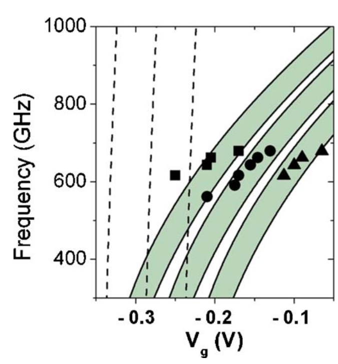

FIG. 3. (Color online) Maxima of resonant gate voltages corresponding to different frequencies of the radiation source at three different fixed drain-to-source voltages [(■): 0.1 V, (●): 0.2 V, and (▲): 0.3 V]. Dashed lines, respectively, from left to right are calculations using Eqs. (2) and (3) for three values of the effective threshold voltage $V_{\text{th}'}$ (−0.35, −0.3, and −0.25 V) corresponding to three values of applied V_d (0.1, 0.2, and 0.3 V). Electron velocity is assumed to be 2×10^5 m s^{-1}. Solid lines are calculations using Eq. (4) at two different values of electron drift velocity (2×10^5 and 3.5×10^5 m/s) for each effective threshold voltage (i.e., $V_{\text{th}'}$=−0.35, −0.3, and −0.25 V). Filled areas represent drift velocity range (between 2×10^5 and 3.5×10^5 m/s) which can match observed frequency dependence as a function of gate voltage.

length L_g, the plasma wave velocity s, and drift velocity ν as[19,20]

$$f=\frac{s}{4L_g}\left(1-\frac{v^2}{s^2}\right), \tag{2}$$

with

$$s=\sqrt{\frac{e}{m^*}V_0}, \tag{3}$$

where e is the electron charge and m^* is the effective electron mass. The effective gate-to-channel voltage swing[21] V_0, can be estimated from the formula $V_0 \approx V_g - V_{\mathrm{th}'} = V_g - \{V_{\mathrm{th}} - (I_d R_s/2) - (V_{\mathrm{ch}}/2)\}$, where V_g is the external gate voltage, $V_{\mathrm{th}}=-0.4$ V is the threshold voltage, I_d is the drain current, R_s is the total source series resistance, and V_{ch} is the voltage drop on the gated part of the channel. The total source-drain voltage can be written as $V_d = V_{\mathrm{ch}} + I_d R_s$. Since $L_g + 2d < L_{sd}$ (d is the thickness of the wide band barrier, $d=17$ nm so $L_g+2d=84$ nm and $L_{sd}=1.4$ μm is the drain-source separation), most of the source-drain voltage drop in the linear region occurs across R_s determined by the source-gate and drain-gate access regions. Therefore, V_{ch} can be neglected. In our case, as we use $V_d=0.1$, 0.2, and 0.3 V, the effective threshold voltage can be estimated from $V_{\mathrm{th}'} \approx V_{\mathrm{th}} + (V_d/2) = -0.35$, -0.3, and -0.25 V, respectively.

Dashed lines in Fig. 3 are calculations using Eqs. (2) and (3) taking $V_0 \approx V_{gs} - V_{\mathrm{th}'}$ as fitting parameter to describe resonant peak shifting with applied V_d. The electron drift velocity in the saturation regime is assumed to be 2×10^5 m/s. One can see that calculation does not reproduce well the increase of the gate voltage with frequency. The quantitative interpretation based on these equations allows us to get only approximate description of experimental data. In fact, the transistor channel region under the gate cannot be considered as separated from the other parts of the transistor. The transistor consists not only on the gated part but also on the ungated part that is covered by the cap layer. In the condition of strong current, the plasma frequency can be modified by the interaction of plasma oscillations in different parts of the channel. The importance of the cap layer regions was theoretically discovered by Ryzhii *et al.*[22]

As predicted in Ref. 22 the cap regions significantly affect the plasma oscillation spectrum in HEMTs: the resonant plasma frequencies dramatically decrease with increasing cap region length. In order to take into account the effect of such cap layers, a correction to the Eq. (2) gives

$$f \approx \frac{s}{2(L_g+L_c)}\left(1-\frac{v^2}{s^2}\right), \tag{4}$$

where L_c is the cap layer length.

Solid lines in Fig. 3 are calculations using Eq. (4) at two different values of electron drift velocity (2×10^5 and 3.5×10^5 m/s) for each effective threshold voltage used before (i.e. $V_{\mathrm{th}'}=-0.35$, -0.3, and -0.25 V). Filled areas represent drift velocity range (between 2×10^5 and $3.5\ 10^5$ m/s) which can match observed frequency dependence as a function of gate voltage. The effect of cap layer result in a significant reduction of the frequencies in comparison with those calculated for the simplified HEMTs model Eq. (1). The calculated increases of frequency with gate voltage can now be qualitatively explained. However, the existing theory concerns the transistor working in the linear part of the $I(V)$ characteristics and the resonant detection is observed in the saturation region only, where the carrier density and velocity are not uniform in the whole channel. We want to stress that the strict theory for a nonuniform drift velocity distribution along the channel and more quantitative description of the phenomenon in the saturation region are absent so far. A full quantitative interpretation of our results requires a more complete theoretical development.

In conclusion we have experimentally shown that the room temperature resonant detection of subterahertz electromagnetic waves in InGaAs nanometric HEMTs can be tunable with gate voltage. The physical mechanism of the detection is related to the plasma waves excited in the transistor channel. We have also shown that the cap layer regions significantly affect the plasma oscillation spectrum in HEMTs.

The research at Montpellier2 University was supported by ACI "Tera-Nano," by the French Ministry of Scientific Research, and by the CNRS European Research Group (GdR-E) "Solid State Detectors and Emitters of Terahertz Radiation."

[1] M. Kroug, S. Cherednichenko, H. Merkel, E. Kollberg, B. Voronov, G. Gol'tsman, H. W. Huebers, and H. Richter, IEEE Trans. Appl. Supercond. **11**, 962 (2001).
[2] P. J. Burke, R. J. Schoelkopf, D. E. Prober, A. Skalare, B. S. Karasik, M. C. Gaidis, W. R. McGrath, B. Bumble, and H. G. LeDuc, J. Appl. Phys. **85**, 1644 (1999).
[3] B. S. Karasik, W. R. McGrath, M. E. Gershenson, and A. V. Sergeev, J. Appl. Phys. **87**, 7586 (2000).
[4] T. W. Crow, R. J. Mattauch, R. M. Weikle, U. V. Bhapkar, in *Compound Semiconductor Electronics*, edited by M. Shur (World Scientific, Singapore, 1996), p. 209.
[5] S. M. Marazita, W. L. Bishop, J. L. Hesler, K. Hui, W. E. Bowen, and T. W. Crowe, IEEE Trans. Electron Devices **47**, 1152 (2000).
[6] E. E. Haller and J. W. Beeman, Proceedings of Far-IR, Sub-mm & mm Detector Technology Workshop, Vol. 4857, Monterey, CA, April 2002.
[7] G. E. Stillman, C. M. Wolfe, and J. O. Dimmock, Solid State Commun. **7**, 5 (1969).
[8] G. Strasser, K. Bochter, M. Witzany, and E. Gornik, Infrared Phys. **32**, 439 (1991).
[9] A. V. Chaplik, Zh. Eksp. Teor. Fiz. **62**, 746 (1972) [Sov. Phys. JETP **35**, 395 (1972)].
[10] M. Dyakonov and M. S. Shur, the Proceedings of 22nd International Symposium on GaAs and Related Compounds, Cheju, Korea, 28 August 1–September 1995 (unpublished), Institute Conference Series No. 145, Chap. 5, pp. 785–790.
[11] M. Dyakonov and M. S. Shur in *Terahertz Sources and Systems*, edited by R. E. Miles (Kluwer, Netherlands, 2001), pp. 187–207.
[12] M. Dyakonov and M. Shur, Phys. Rev. Lett. **71**, 2465 (1993).
[13] M. Dyakonov and M. S. Shur, Phys. Rev. Lett. **71**, 2465 (1993); IEEE Trans. Electron Devices **43**, 380 (1996).
[14] W. Knap, Y. Deng, S. Rumyantsev, and M. S. Shur, Appl. Phys. Lett. **81**, 4637 (2002).
[15] W. Knap, Y. Deng, S. Rumyantsev, J.-Q. Lu, M. S. Shur, C. A. Saylor, and L. C. Brunel, Appl. Phys. Lett. **80**, 3433 (2002).
[16] T. Otsuji, M. Hanabe, and O. Ogawara, Appl. Phys. Lett. **85**, 2119 (2004).
[17] X. G. Peralta, S. J. Allen, M. C. Wanke, N. E. Harff, J. A. Simmons, M. P. Lilly, J. L. Reno, P. J. Burke, and J. P. Eisenstein, Appl. Phys. Lett. **81**, 1627 (2002).
[18] E. A. Shaner, Mark Lee, M. C. Wanke, A. D. Grine, J. L. Reno, and S. J. Allen, Appl. Phys. Lett. **87**, 193507 (2005).
[19] F. Teppe, W. Knap, D. Veksler, M. Shur, A. P. Dmitriev, V. Y. Kachorovskii, and S. Rumyantsev, Appl. Phys. Lett. **87**, 052107 (2005).
[20] D. Veksler, F. Teppe, A. P. Dmitriev, V. Y. Kachorovskii, W. Knap, and M. Shur, Phys. Rev. B **73**, 125328 (2006).
[21] W. Knap, J. Lusakowski, T. Parenty, S. Bollaert, A. Cappy, V. V. Popov, and M. S. Shur, Appl. Phys. Lett. **84**, 2331 (2004).
[22] V. Ryzhii, A. Satou, W. Knap, and M. S. Shur, J. Appl. Phys. **99**, 084507 (2006).